

ATP-binding cassette transporter A7 enhances phagocytosis of apoptotic cells and associated ERK signaling in macrophages

Andreas W. Jehle,¹ Shyra J. Gardai,^{3,4} Suzhao Li,¹ Patrick Linsel-Nitschke,¹ Konosuke Morimoto,³ William J. Janssen,³ R. William Vandivier,³ Nan Wang,¹ Steven Greenberg,^{1,2} Benjamin M. Dale,² Chunbo Qin,⁵ Peter M. Henson,⁴ and Alan R. Tall¹

¹Department of Medicine and ²Department of Pharmacology, Columbia University, New York, NY 10032

³Division of Pulmonary Sciences and Critical Care Medicine, Department of Medicine, University of Colorado Health Sciences Center, Denver, CO 80262

⁴Program in Cell Biology, the Department of Pediatrics, National Jewish Medical and Research Center, Denver, CO 80206

⁵Department of Biochemistry, Weill Medical College of Cornell University, New York, NY 10021

The mammalian ATP-binding cassette transporters A1 and A7 (ABCA1 and -A7) show sequence similarity to CED-7, a *Caenorhabditis elegans* gene that mediates the clearance of apoptotic cells. Using RNA interference or gene targeting, we show that knock down of macrophage ABCA7 but not -A1 results in defective engulfment of apoptotic cells. In response to apoptotic cells, ABCA7 moves to the macrophage cell surface and colocalizes with the low-density lipoprotein receptor-related protein 1 (LRP1) in phagocytic cups. The cell sur-

face localization of ABCA7 and LRP1 is defective in ABCA7-deficient cells. C1q is an opsonin of apoptotic cells that acts via phagocyte LRP1 to induce extracellular signal-regulated kinase (ERK) signaling. We show that ERK signaling is required for phagocytosis of apoptotic cells and that ERK phosphorylation in response to apoptotic cells or C1q is defective in ABCA7-deficient cells. These studies reveal a major role of ABCA7 and not -A1 in the clearance of apoptotic cells and therefore suggest that ABCA7 is an authentic orthologue of CED-7.

Introduction

Apoptosis is a critical process in development and normal tissue homeostasis and results in immediate removal of dying cells, either by neighboring cells or by professional phagocytes, such as macrophages or dendritic cells. The engulfment of apoptotic cells is one of the most primitive forms of phagocytosis, and many of the molecules implicated in the phagocytosis of apoptotic cells appear to have a high degree of conservation from the nematode *Caenorhabditis elegans* to mammalian cells (Henson et al., 2001). Phagocytosis of apoptotic cells is distinguished from the evolutionarily much younger Fc receptor (FcR)-mediated phagocytosis in terms of receptors, signaling molecules, and cytoskeletal as well as plasma membrane reorganizations (Aderem and Underhill, 1999).

In *C. elegans*, at least two partially redundant processes are important in the engulfment of dying cells, one that involves CED-2, -5, and -12 and another involving CED-7, -1, and -6,

and subsequently both pathways converge at CED-10 (Kinchen et al., 2005). In the second pathway, CED-7 may be required for the function of CED-1 (Wu and Horvitz, 1998), although recent data indicate that CED-7 may have alternative roles during the removal of apoptotic cells (Kinchen et al., 2005). For all of these ced genes, mammalian orthologues have been proposed (for review see Reddien and Horvitz, 2004). For CED-7, the ATP-binding cassette transporter A1 (ABCA1) has been suggested as the mammalian orthologue, based on sequence conservation and in vivo and cell culture studies suggesting a role of ABCA1 in the phagocytosis of apoptotic cells (Luciani and Chimini, 1996; Marguet et al., 1999; Hamon et al., 2000). The low-density lipoprotein receptor-related protein 1 (LRP1) or CD91 has been suggested as a protein with function similar to CED-1 (Su et al., 2002). LRP1 is a multifunctional scavenger and signaling receptor (Herz and Strickland, 2001). The suggestion that LRP1 has a function similar to CED-1 is based on intracellular sequence similarity and an important role of LRP1 in the phagocytosis of apoptotic cells (Ogden et al., 2001; Vandivier et al., 2002; Gardai et al., 2003, 2005). Moreover, both LRP1 and CED-1 can interact via a phosphotyrosine binding motif

Correspondence to Andreas W. Jehle: aj2115@columbia.edu

Abbreviations used in this paper: ABCA1, ATP-binding cassette transporter A1; apoA-I, apolipoprotein A-I; ERK, extracellular signal-regulated kinase; FcR, Fc receptor; LPS, lipopolysaccharide; PI, phagocytic index.

The online version of this article contains supplemental material.

(NPXY motif) within their cytoplasmic tails with the adaptor proteins CED-6 and its mammalian orthologue GULP (engulfment adaptor protein), respectively (Su et al., 2002). However, LRP1 and CED-1 show very limited overall sequence homology, and it is possible that the apparent similarity in their functions represents convergent evolution.

ABCA7, a close homologue of ABCA1, is a 220-kD protein expressed in a variety of tissues, including macrophages (Wang et al., 2003). We have shown that ABCA7 binds apolipoprotein A-I (apoA-I) and promotes the efflux of phospholipids but not cholesterol to apoA-I in ABCA7-transfected 293 cells. In resting macrophages, ABCA7 is found intracellularly and does not contribute to phospholipid or cholesterol efflux (Kim et al., 2005; Linsel-Nitschke et al., 2005). The physiological role of ABCA7 in these cells remains unknown.

In this paper, we show that ABCA7 has a high sequence similarity to CED-7 and is required for efficient phagocytosis of apoptotic cells. We were unable to demonstrate a role of ABCA1 in the phagocytosis of apoptotic cells as reported previously (Luciani and Chimini, 1996; Hamon et al., 2000). ABCA7 appears to facilitate the cell surface localization of LRP1 and associated signaling via extracellular signal-regulated kinase (ERK), thereby promoting the phagocytosis of apoptotic cells. Together, these data suggest that ABCA7 and not -A1 is a functional orthologue of CED-7.

Results

Sequence similarity of ABCA7 and CED-7

An alignment of CED-7 and mouse ABCA7 showed that 25% of amino acids were identical and 43% were similar. A similar result was obtained if CED-7 was aligned to mouse ABCA1, resulting in 24% identity and 42% similarity. These homologies are in the range reported for known orthologous proteins (e.g., CED-6 and GULP; Su et al., 2002). Compared with ABCA1 and -A7, CED-7 has a gap in the amino acid sequence starting at amino acid 198 (Fig. S1 a, available at <http://www.jcb.org/cgi/content/full/jcb.200601030/DC1>). This difference is more pronounced for ABCA1 (Fig. S1 b, dashed line). No other mammalian genes are more homologous to CED-7 than ABCA7 or -A1. Based on these sequence similarities, both ABCA7 and -A1 could be considered as potential orthologues to CED-7; thus, we undertook a study of the function of ABCA7 in the phagocytosis of apoptotic cells.

Localization of ABCA7 in membrane ruffles and phagocytic cups

The first observation indicating that ABCA7 might be involved in phagocytosis came from fluorescence microscopy experiments. We previously reported that “resting” macrophages show mainly intracellular staining for ABCA7 (Linsel-Nitschke et al., 2005). We confirmed this finding by confocal microscopy and saw mainly intracellular staining for ABCA7 (Fig. 1 a). Some cells also showed staining for ABCA7 at the leading edge (Fig. 1 a, solid arrows). Affinity-purified preimmune serum showed no staining in macrophages. Colocalization studies in resting macrophages indicated partial overlap of ABCA7 with the

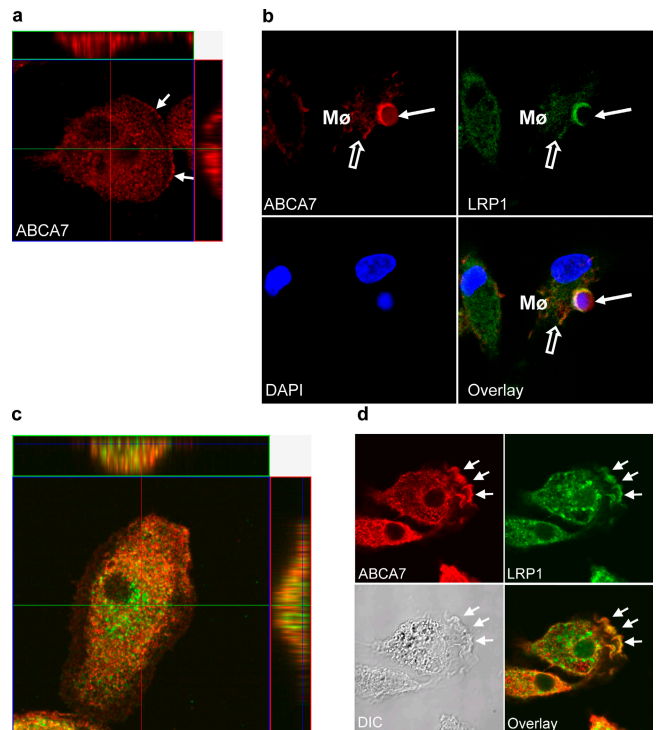


Figure 1. ABCA7 and LRP1 colocalize in the phagocytic cup and in membrane ruffles. (a) ABCA7 in resting macrophages. Mouse peritoneal macrophages were cultured for 2 d before fixation, permeabilization, and incubation with peptide affinity column purified antibody against ABCA7 (red). Confocal image with orthographic projection shows mainly intracellular staining for ABCA7. (b) Confocal picture showing a macrophage (Mφ; open arrows) engulfing an apoptotic cell (solid arrows). The top left panel shows localization of ABCA7 in the phagocytic cup. The top right panel shows localization of LRP1 in the phagocytic cup. In the overlay (bottom left), the colocalization of ABCA7 and LRP1 within the phagocytic cup is shown in yellow. (c) Confocal image showing staining for ABCA7 and LRP1 in resting macrophages. The staining for ABCA7 (red) and LRP1 (green) was mainly intracellular with very limited colocalization. (d) Differential interference contrast (DIC) microscope image (bottom left) and immunofluorescence images showing colocalization of ABCA7 and LRP1 mainly within membrane ruffles (solid arrows) after stimulation of macrophages with 10 μg/ml C1q for 20 min.

Golgi marker Golgi 58K and an early endosome marker (rab4; unpublished data). The distribution of ABCA7 altered in macrophages undergoing phagocytosis with redistribution of ABCA7 into phagocytic cups (Fig. 1 b, top left) and enrichment in membrane ruffles (Fig. 1 d, top left, solid arrows). This redistribution of ABCA7 was not specific for phagocytosis of apoptotic cells, as it was also seen with IgG-coated latex beads fed to J774 macrophages (Fig. S2, bottom left, arrows; available at <http://www.jcb.org/cgi/content/full/jcb.200601030/DC1>).

ABCA7 colocalizes with LRP1 within the phagocytic cup

Based on the report that CED-7, a possible orthologue of ABCA7, may be required for the function of CED-1 (Wu and Horvitz, 1998) and the suggestion that LRP1 could have a function similar to CED-1 (Su et al., 2002), we also compared the localization and functions of ABCA7 and LRP1. Studies in “resting” macrophages showed very little colocalization of ABCA7 (Fig. 1 c, red) and LRP1 (green). However, confocal

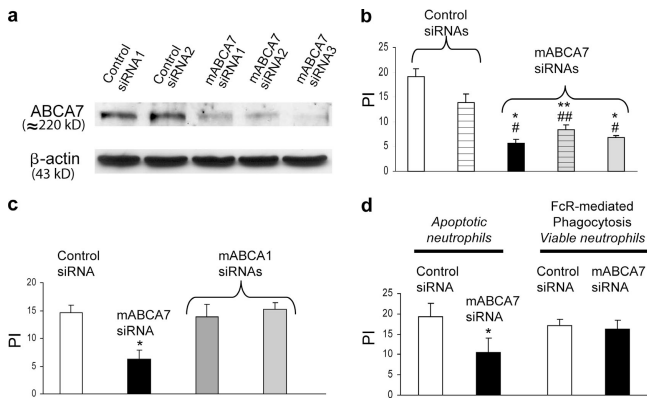


Figure 2. Knock down of ABCA7 reduces phagocytosis of apoptotic cells but has no effect on FcR-mediated phagocytosis. (a) Mouse peritoneal macrophages were transfected with either control siRNA or three different siRNAs directed against ABCA7, and total cell lysates were subjected to Western immunoblotting using antibodies against ABCA7 and β -actin. Densitometric analysis of bands showed a 60–80% reduction of ABCA7 protein with the different siRNA constructs. (b) Phagocytosis of apoptotic cells experiment using the siRNA constructs from panel a. Peritoneal macrophages in a 24-well plate were incubated for 90 min with 10^6 apoptotic neutrophils, and wells were washed, fixed, and stained followed by analysis of PI. Two different scrambled (controls) and three different siRNAs directed against ABCA7 (black bar, gray bar with horizontal lines, and gray bar) were used. $n = 3$; *, $P < 0.001$; **, $P < 0.01$ when compared with control siRNA1 (white bar); #, $P < 0.01$; ##, $P = 0.02$ when compared with control siRNA2 (white bar with horizontal lines). (c) Using control siRNA (white bar), ABCA7 siRNA (black bar), and two different siRNAs directed against ABCA1 (dark gray and light gray bars), a significant reduction of PI was seen with knock down of ABCA7 ($n = 3$; *, $P = 0.005$), whereas knock down of ABCA1 had no effect. (d) To compare phagocytosis of apoptotic cells with FcR-mediated phagocytosis, either apoptosis was induced by UV radiation or viable neutrophils were coated with a monoclonal anti-CD18 antibody. White and black bars represent the PI of cells transfected with control or ABCA7 siRNA, respectively. The knockdown of ABCA7 only reduced phagocytosis of apoptotic cells ($n = 4$; *, $P = 0.02$) and had no effect on FcR-mediated phagocytosis.

microscopy of macrophages (Fig. 1 b, open arrows) engulfing an apoptotic cell showed that ABCA7 (red) and LRP1 (green) colocalized within the phagocytic cup (solid arrow), as shown by the yellow in the overlay. Colocalization of ABCA7 and LRP1 was also observed within membrane ruffles after activation of macrophages by C1q (Fig. 1 d, bottom right).

Knock down of ABCA7 reduces phagocytosis of apoptotic cells but has no effect on FcR-mediated phagocytosis

To test whether ABCA7 is of functional relevance in phagocytosis, we performed genetic knockdown experiments of ABCA7 in mouse peritoneal macrophages. Six different siRNA constructs complementary to ABCA7 were tested to down-regulate ABCA7. The best three constructs were used in subsequent experiments. Each of them suppressed ABCA7 by ~60–80% (Fig. 2 a). The control siRNAs did not affect ABCA7 protein expression (unpublished data). Fig. 2 b shows that all three siRNA constructs for ABCA7 significantly inhibited the phagocytosis of apoptotic cells by 60–70%. Knock down of ABCA7 did not impair binding of apoptotic cells to macrophages (unpublished data). In some experiments, the second control siRNA (control siRNA2; Fig. 2 b, white column with horizontal lines)

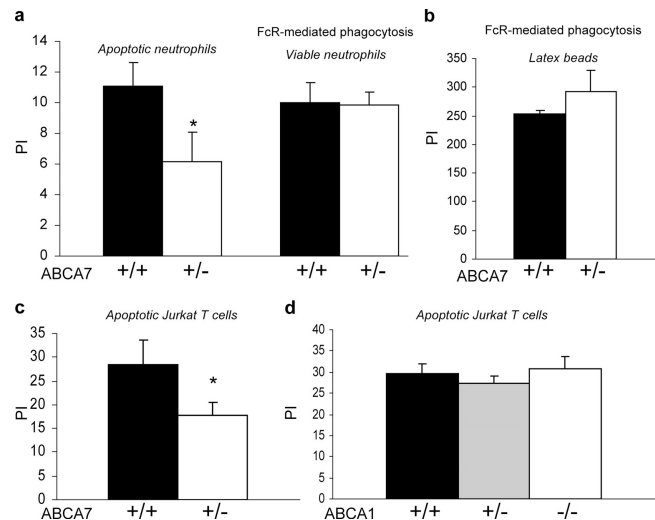


Figure 3. Phagocytosis of apoptotic cells is reduced in ABCA7 +/- compared with ABCA7 +/+ but not in ABCA1 +/- or -/- mice. (a) Uptake of apoptotic neutrophils was reduced 41% in macrophages from ABCA7 +/- compared with macrophages from ABCA7 +/+ mice ($n = 8$; *, $P < 0.001$), whereas there was no difference for FcR-mediated phagocytosis performed in parallel with viable neutrophils coated with a monoclonal anti-CD18 antibody. For all experiments, mouse peritoneal macrophages were harvested and cultured for 2 d before phagocytosis assays were performed. (b) FcR-mediated phagocytosis with 4- μ m IgG-coated latex beads. Compared with the uptake of apoptotic or anti-CD18 antibody labeled viable neutrophils, the PI was much higher (273 ± 33) with the smaller IgG-coated latex beads. Uptake was similar for ABCA7 +/+ and +/- macrophages ($n = 3$; $P = 0.3$). (c) Phagocytosis of apoptotic cells was also performed with apoptotic Jurkat T cells. PI for the ABCA7 +/- was reduced by 39% compared with wild-type control (ABCA7 +/+, $n = 3$; ABCA7 +/-, $n = 5$; *, $P = 0.015$). (d) No difference was found in the uptake of apoptotic Jurkat T cells by macrophages with different genotypes for ABCA1 (ABCA1 +/+, $n = 3$; ABCA1 +/-, $n = 3$; ABCA1 -/-, $n = 3$).

also slightly reduced the phagocytic index (PI). Therefore, for further experiments the first control siRNA (control siRNA1) was used.

As it has been suggested that ABCA1 plays a role in phagocytosis of apoptotic cells (Hamon et al., 2000), we also compared the relative importance of ABCA7 and -A1 in this process. Surprisingly, the knock down of ABCA1 did not decrease the phagocytosis of apoptotic cells (Fig. 2 c), even though the siRNA constructs used for ABCA1 were as effective as the constructs used for ABCA7 (reduction of ABCA1 protein by 60–80%; Fig. S3, available at <http://www.jcb.org/cgi/content/full/jcb.200601030/DC1>). We further tested the effect of genetic suppression of ABCA7 on FcR-mediated phagocytosis. Even though ABCA7 localizes in phagocytic membranes during uptake of IgG-coated latex beads (Fig. S2), down-regulation of ABCA7 had no effect on FcR-mediated phagocytosis (Fig. 2 d).

Phagocytosis of apoptotic cells is also reduced in macrophages from ABCA7 +/- mice

We have obtained mice with a targeted deletion of the ABCA7 gene in exon 21. In contrast to the recently published ABCA7 knockout mouse, created using a different targeting strategy

(Kim et al., 2005), we have not obtained any viable ABCA7 $-/-$ mice. Although we do not know the reason for this discrepancy, a difference in the genetic background of the mice is unlikely, as we were unable to obtain ABCA7 $-/-$ mice in either the C57Bl6 (87 animals screened) or in a C57Bl6 \times 129 F2 hybrid background (23 mice screened: 7 $+/+$, 16 $+/-$, and 0 $-/-$). Thus, we used ABCA7 $+/-$ mice for the experiments. As we demonstrated previously, peritoneal macrophages from ABCA7 $+/-$ mice showed a 50–60% reduction in ABCA7 protein levels (Linsel-Nitschke et al., 2005). Phagocytosis of apoptotic neutrophils was reduced by 41% in macrophages from ABCA7 $+/-$ mice (Fig. 3 a), and similar results were obtained with apoptotic Jurkat T cells (Fig. 3 c). In contrast, macrophages from ABCA7 $+/-$ animals had no defect in the FcR-mediated phagocytosis of viable neutrophils (Fig. 3 a) or IgG-coated latex beads (Fig. 3 b). We also compared the phagocytosis of apoptotic cells in ABCA1 $+/+$, $+/-$, and $-/-$ macrophages. As shown in Fig. 3 d, no difference could be detected between the ABCA1 $+/+$, $+/-$, and $-/-$ mice.

In regard to ABCA1, our data contradict earlier work that reported a role of ABCA1 in the phagocytosis of apoptotic cells (Luciani and Chimini, 1996; Hamon et al., 2000). Therefore, we repeated the phagocytosis assays using a different microscopic method that counts red (prelabeled) apoptotic cells (Fig. 4 a) within green-labeled LAMP1-positive phagolysosomes to score phagocytosis. Using this phagocytosis assay, we found that phagocytosis of apoptotic cells was reduced by 39% in ABCA7 $+/-$ macrophages compared with ABCA7 $+/+$ control cells (Fig. 4 b), but ABCA1 $-/-$ macrophages did not show a defect in phagocytosis (Fig. 4 c). Thus, using two different genetic approaches and two different microscopic phagocytosis assays, we found an essential role of ABCA7 in phagocytosis of apoptotic cells but not in FcR-mediated phagocytosis and no comparable function of ABCA1.

A specific defect in the phagocytosis of apoptotic cells but not in FcR-mediated phagocytosis makes it unlikely that ABCA7 has a general role in the reorganization of the cytoskeleton. A significant general defect could be excluded further, as no difference in membrane ruffling was seen after stimulation of ABCA7 $+/+$ and $+/-$ macrophages (Fig. S4, available at <http://www.jcb.org/cgi/content/full/jcb.200601030/DC1>).

ABCA7 plays a role in phagocytosis of apoptotic cells in vivo

To test whether the clearance of apoptotic cells is also diminished in ABCA7-deficient mice, we used two established in vivo models of phagocytosis. In the first model (Teder et al., 2002; Vandivier et al., 2002), we assessed the clearance of exogenously instilled apoptotic cells in the lungs of ABCA7 $+/-$ and $+/+$ mice. Mice were challenged intratracheally with exogenous apoptotic cells, and clearance was assessed by bronchoalveolar lavage. In this model, defective phagocytosis of apoptotic cells is suggested either by decreased uptake by alveolar macrophages (i.e., decreased PI) or by increased recovery of apoptotic cells in the lavage (Teder et al., 2002; Vandivier et al., 2002). ABCA7 $+/-$ mice showed a significant reduction in the PI (Fig. 5 a). There was also a trend toward an increased

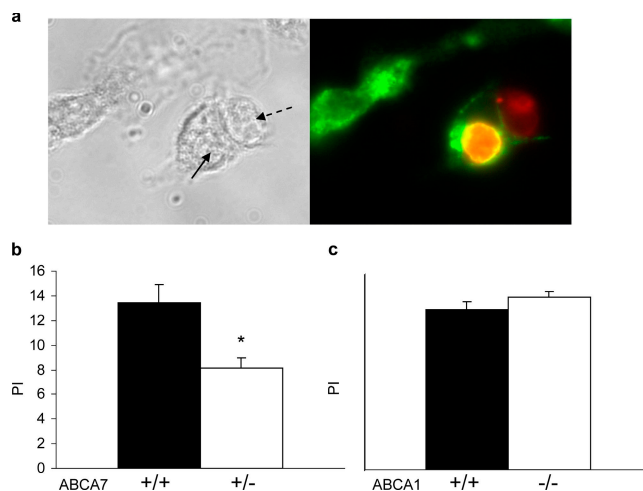


Figure 4. Uptake of apoptotic Jurkat T cells in LAMP1-positive phagolysosomes is reduced in ABCA7 $+/-$ macrophages but not in ABCA1 $-/-$ macrophages. Mouse peritoneal macrophages were incubated with CellTracker red prelabeled apoptotic Jurkat T cells for 45 min before fixation, permeabilization, and incubation with an antibody against LAMP1 (green). (a) Representative phase-contrast picture (left) with corresponding fluorescent photomicrograph (right). The macrophage on the right side engulfed one Jurkat T cells (solid arrow), as indicated by the yellow ring structure in the overlay. A second Jurkat T cell (dashed arrow) binds to the same macrophage and is clearly not within a LAMP1-positive compartment. (b) Uptake of apoptotic Jurkat T cells in LAMP1-positive phagolysosomes was reduced by 39% in ABCA7 $+/-$ macrophages compared with ABCA7 $+/+$ macrophages ($n = 4$; *, $P < 0.001$). (c) There was no difference in the uptake of apoptotic Jurkat T cells in LAMP1-positive phagolysosomes by macrophages with different genotypes for ABCA1 (mean and SD of triplicate experiments of two pairs of ABCA1 $+/+$ and $-/-$ mice).

recovery of apoptotic cells for ABCA7 $+/-$ mice compared with their $+/+$ age-matched controls (Fig. 5 b). In the second in vivo model, ABCA7 $+/-$ and $+/+$ mice were challenged intratracheally with lipopolysaccharide (LPS), and the inflammatory response and the clearance of endogenous apoptotic cells was assessed by bronchoalveolar lavage at day 0 (control group without LPS) and 3 d after LPS instillation. Without LPS (day 0), the PI was small and no significant difference between groups was observed (PI for ABCA7 $+/+$, 1.0 ± 0.6 [$n = 6$]; PI for ABCA7 $+/-$, 0.6 ± 0.4 [$n = 4$]). However, 3 d after LPS instillation, the PI was increased and was significantly smaller in the ABCA7 $+/-$ mice compared with their $+/+$ age-matched controls (Fig. 5 c). Total numbers of cells in the bronchoalveolar lavage fluids as well as the differential white cell count at baseline and after LPS were similar for ABCA7 $+/+$ and $+/-$ mice (unpublished data).

ABCA7 facilitates the cell surface expression of ABCA7 and LRP1 after stimulation with apoptotic cells or C1q

In the experiments described so far, we have shown that ABCA7, like LRP1 (Ogden et al., 2001), is required for the phagocytosis of apoptotic cells but not for FcR-mediated phagocytosis. Further, we have shown that both ABCA7 and LRP1 are redistributed from an intracellular pool to the phagocytic cup (an extension of the plasma membrane) during phagocytosis (Fig. 1 b). We next asked whether there might be a defect in cell surface

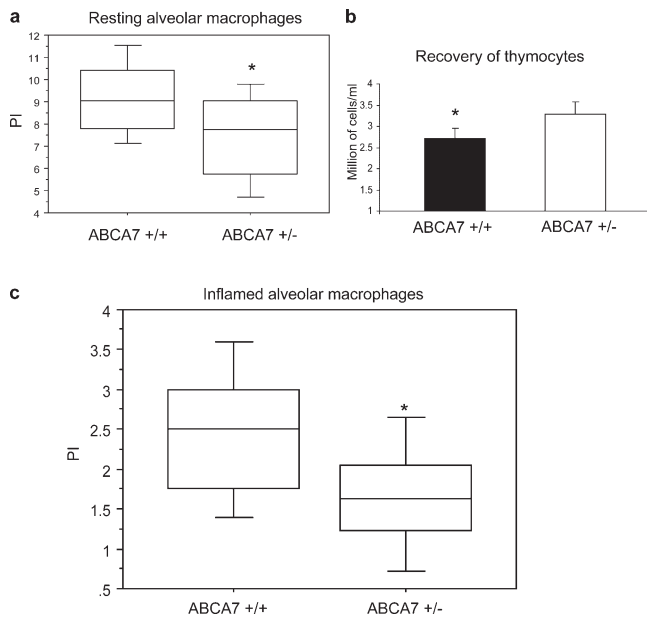


Figure 5. ABCA7 +/- mice show a phagocytosis defect in vivo. (a) Decreased uptake of apoptotic cells by resting (not inflamed) alveolar macrophages. 10×10^6 apoptotic thymocytes were instilled intratracheally. 1 h later, whole lung lavage was performed, followed by analysis of the alveolar macrophage PI. The figure shows a box blot (with 90, 75, 50, 25, and 10 percentile values of PI) for 10 ABCA7 +/+ mice and a box blot for 9 ABCA7 +/- mice (in one ABCA7 +/- mouse, the trachea was accidentally perforated, and this mouse was excluded from analysis). The mean PI was significantly lower for ABCA7 +/- mice. *, $P = 0.049$. (b) Same experiment as in panel a: from the whole lavage, the recovery of apoptotic thymocytes was also determined. The mean recovery in ABCA7 +/- mice (black bar with SEM) tended to be slightly lower than for ABCA7 +/- mice (white bar with SEM; *, $P = 0.13$). (c) Decreased phagocytosis of LPS-induced apoptotic cells by inflamed alveolar macrophages. 3 d after 200 mcg LPS was instilled into the lungs, lung lavage was performed, followed by analysis of the alveolar macrophage PI. The figure shows a box blot (with 90, 75, 50, 25, and 10 percentile values of PI) for 10 ABCA7 +/+ mice and a box blot for 8 ABCA7 +/- mice. The mean PI was significantly lower for ABCA7 +/- mice. *, $P = 0.046$.

expression of ABCA7 and LRP1 during phagocytosis in ABCA7 +/- macrophages. As the movement of ABCA7 and LRP1 to the cell surface during phagocytosis is difficult to quantitate by microscopy, we developed a biochemical assay, i.e., cell surface biotinylation followed by pull down with streptavidin beads and immunoblotting for ABCA7 and LRP1. Fig. 6 a shows a 12-fold and sustained enrichment in cell surface levels of ABCA7 and a fourfold, more transient increase of cell surface LRP1 in ABCA7 +/+ macrophages after exposure to apoptotic cells. The enrichment of ABCA7 and LRP1 was markedly attenuated in ABCA7 +/- macrophages (2.5-fold for ABCA7 and 1.5–2-fold for LRP1; Fig. 6 a, representative result of three independent experiments). Overall levels of LRP1 and ABCA7 in cell lysates were not affected by the uptake of apoptotic cells (unpublished data).

An early event during phagocytosis is binding of C1q on apoptotic cells to calreticulin/LRP1 on phagocytes, leading to signaling and uptake of apoptotic cells (Ogden et al., 2001). To see if the interaction of C1q with LRP1 was sufficient to induce cell surface expression of ABCA7, macrophages were serum starved and then exposed to C1q. Consistent with the earlier result showing C1q-induced appearance of ABCA7 in

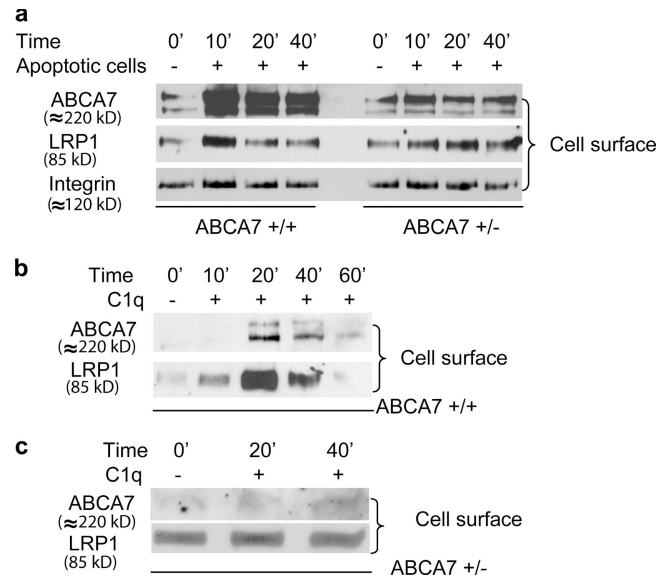


Figure 6. ABCA7 facilitates cell surface expression of ABCA7 and LRP1 after stimulation with apoptotic cells or after stimulation with C1q. (a) Cell surface levels of ABCA7 and LRP1 in phagocytes after exposure to apoptotic cells. Apoptotic Jurkat T cells were added to monolayers of ABCA7 +/+ and +/- macrophages. At the indicated time points, apoptotic cells were removed and macrophages were washed and biotinylated on ice, and biotinylated proteins were recovered with streptavidin beads and processed for immunoblotting. Recovery of biotinylated proteins was monitored by Ponceau staining of membranes or by Western blotting for integrin β1. A representative experiment of three experiments is shown. (b) Before stimulation of macrophages with 10 μg/ml C1q, cells were incubated in serum-free DME for 3–4 h. At the indicated time points, ABCA7 +/+ macrophages were biotinylated on ice and processed as described above. Results are representative of six similar experiments. (c) At the indicated time points after the addition of C1q, ABCA7 +/- macrophages were biotinylated on ice and processed as described above. Results are representative of five different experiments.

membrane ruffles (Fig. 1 d), this led to a substantial increase in cell surface expression levels of both ABCA7 and LRP1 (Fig. 6 b, representative result of six independent experiments). In ABCA7 +/- cells, the increase in ABCA7 was greatly reduced, and LRP1, although readily detectable in the cell surface, showed minimal response to C1q treatment (Fig. 6 c). This suggests that the increased cell surface expression of ABCA7 and LRP1 in membrane ruffles and during phagocytosis of apoptotic cells at least in part depends on signaling through LRP1 as well as on ABCA7 function. The failure to detect a substantial increase of ABCA7 and LRP1 in the cell surface in ABCA7 +/- cells after stimulation may in part result from a relatively high constitutive cell surface expression of these molecules.

Phosphorylation of ERK is diminished after stimulation with C1q or apoptotic cells in ABCA7 +/- macrophages

As activation of LRP1 by different ligands (Orr et al., 2003; Yang et al., 2004) as well as C1q (unpublished data) leads to phosphorylation of ERK, we tested the signaling function of LRP1 by evaluating ERK phosphorylation after stimulation of macrophages with C1q. As shown in Fig. 7 a, after stimulation with C1q for 10 and 20 min, ERK phosphorylation was reduced by 57 and 65% in ABCA7 +/- macrophages, respectively (similar results

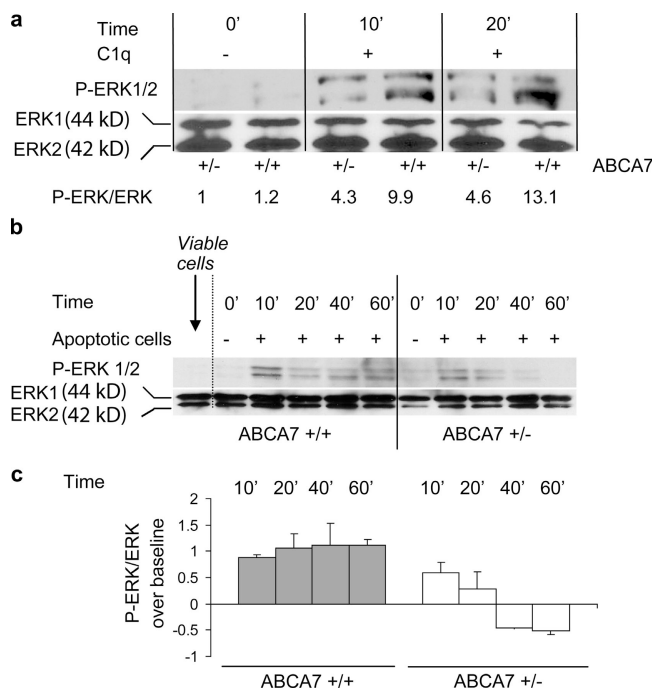


Figure 7. ERK phosphorylation after stimulation with C1q or after addition of apoptotic cells is impaired in macrophages from ABCA7 +/- mice. (A) Time course of ERK phosphorylation after exposure of macrophages to C1q. Before stimulation of macrophages with 10 μ g/ml C1q, cells were incubated in serum-free DME for 3–4 h. At the indicated time points, cells were lysed and lysates were analyzed for phospho-ERK1/2 (P-ERK1/2) and total ERK1/2 by immunoblotting and analyzed by densitometry. Levels of phospho-ERK1/2 were normalized to total ERK1/2 levels and expressed as P-ERK/ERK ratios. Similar results were obtained in three additional experiments. (b) Time course of ERK phosphorylation of exposure of macrophages to apoptotic cells. Apoptotic Jurkat T cells were added to monolayers of ABCA7 +/+ and +/- macrophages. At the indicated time points, apoptotic cells were removed and macrophages were washed before lysis of cells. Immunoblotting was performed as indicated above. (c) Quantification of P-ERK/ERK after stimulation with apoptotic cells. The y axis shows P-ERK/ERK for the indicated time points over baseline (time point 0') expressed as mean and SEM of three independent experiments.

were obtained in four experiments). In contrast, after stimulation of the FcR with aggregated IgG, the magnitude and the time course of ERK phosphorylation were very similar in ABCA7 +/+ and +/- macrophages (Fig. S5, available at <http://www.jcb.org/cgi/content/full/jcb.200601030/DC1>). Macrophages were also stimulated more physiologically by apoptotic cells (Fig. 7, b and c). Apoptotic cells caused a rapid increase in ERK phosphorylation in phagocytes that was sustained to the end of the experiment. Compared with wild-type cells, in ABCA7 +/- cells, basal levels of ERK phosphorylation were slightly higher, there was less initial increase in ERK phosphorylation, and the response was transient, returning to the baseline level after 20–40 min (Fig. 7 c shows quantification of three independent experiments).

Inhibition of ERK phosphorylation reduces phagocytosis of apoptotic cells and prevents the increase of cell surface expression of ABCA7 and LRP1 after stimulation with apoptotic cells

To see whether attenuated ERK phosphorylation in ABCA7 +/- macrophages could explain the decreased phagocytosis of

apoptotic cells, the effect of two inhibitors of ERK phosphorylation on the phagocytosis of apoptotic cells was tested. Viability of macrophages was not affected by the use of inhibitors as assessed by annexin V staining (unpublished data). As shown in Fig. 8 a, both inhibitors reduced phagocytosis of apoptotic cells and C1q-coated apoptotic cells, whereas the effect on FcR-mediated phagocytosis was not significant. This may explain the reduced phagocytosis of apoptotic cells by ABCA7 +/- macrophages, as they show a defect in ERK phosphorylation (Fig. 7, a, b, and c).

Finally, we addressed the question of whether ERK phosphorylation is required for the increased ABCA7 and LRP1 expression at the cell surface upon stimulation with apoptotic cells. Inhibition of ERK prevented the increase of ABCA7 and LRP1 expression at the cell surface after stimulation with apoptotic cells (Fig. 8 b). At baseline (without addition of apoptotic cells), cell surface expression levels of ABCA7 and LRP1 were higher after inhibition of ERK phosphorylation, similar to findings in ABCA7 +/- macrophages, where basal cell surface expression of these molecules was relatively high, but showed only limited increase upon stimulation with apoptotic cells or C1q.

Discussion

The clearance of apoptotic cells occurs throughout the lifespan of multicellular organisms and is important for development during embryogenesis, the maintenance of tissue integrity and function, and the resolution of inflammation (deCathelineau and Henson, 2003). Here, we report that macrophage ABCA7 enhances the clearance of apoptotic cells in vitro and in vivo. ABCA7 and LRP1 move to the cell surface after stimulation with C1q or apoptotic cells and localize to membrane ruffles or phagocytic cups, respectively. However, ABCA7 also localizes to phagocytic membranes during FcR-mediated phagocytosis, in which ABCA7 levels are not rate limiting. More important, ABCA7 is required for optimal ligand-induced signaling through LRP1, as shown by C1q-induced ERK phosphorylation and for sustained ERK phosphorylation during phagocytosis of apoptotic cells. Finally, ERK phosphorylation itself is shown to be essential for phagocytosis of apoptotic cells but not for FcR-mediated phagocytosis, suggesting a link between the defect in ERK phosphorylation and the impaired phagocytosis of apoptotic cells observed in ABCA7 +/- cells.

A variety of different lines of evidence, using siRNA and gene targeted mice, demonstrate a significant role of ABCA7 in the phagocytosis of apoptotic cells. A 60–80% reduction of ABCA7 protein by siRNA resulted in a 60–70% reduction in the phagocytosis of apoptotic cells, and a 50–60% reduction in ABCA7 in ABCA7 +/- mice led to a 40% reduction in the phagocytosis of apoptotic cells, indicating a major role of ABCA7 in this process. By comparison, macrophages treated with antibodies against LRP1, C1q, and mannose binding lectin or in C1q -/- mice, phagocytosis of apoptotic cells is reduced by ~50–75% (Taylor et al., 2000; Ogden et al., 2001). Furthermore, LPS-induced lung inflammation in CD44 -/- mice (Teder et al., 2002; the same model used in this study [Fig. 5 b]) resulted in a reduced PI, similar to that reported here.

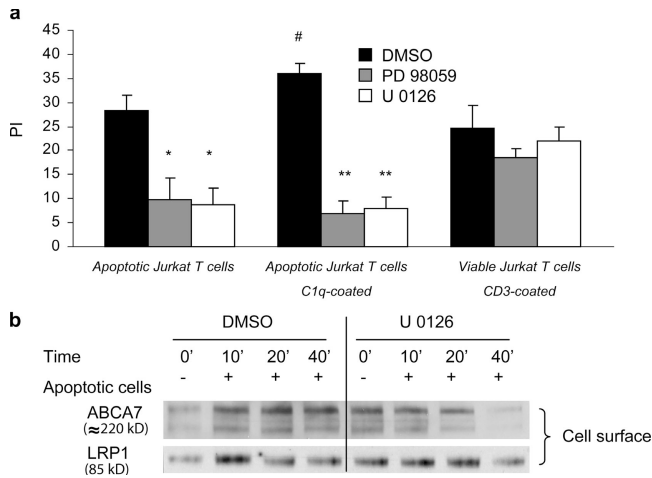


Figure 8. Inhibition of ERK phosphorylation reduces phagocytosis of apoptotic cells and prevents the increase of cell surface expression of ABCA7 and LRP1 after stimulation with apoptotic cells. (a) J774 macrophages in a 24-well plate were preincubated with DMSO, 20 μ M PD 98059, or 10 μ M U 0126 for 20 min, washed, and incubated for 90 min with 10^6 apoptotic Jurkat T cells, C1q-coated apoptotic Jurkat T cells, or viable Jurkat T cells coated with human anti-CD3 antibody. Cells were then washed, fixed, and stained followed by analysis of PI. In the absence of inhibitors, uptake of C1q-coated apoptotic cells increased 20% compared with apoptotic T cells ($n = 3$; #, $P = 0.048$). Inhibition of ERK phosphorylation inhibited uptake of apoptotic cells and C1q-coated apoptotic cells by 75 and 80%, respectively ($n = 3$; *, $P < 0.01$; **, $P < 0.001$), whereas both inhibitors had no significant effect on FcR-mediated phagocytosis (PD 98059, $P = 0.15$; U 0126, $P = 0.54$). (b) Cell surface levels of ABCA7 and LRP1 in phagocytes after inhibition of ERK phosphorylation. Apoptotic Jurkat T cells were added to monolayers of wild-type macrophages, which were preincubated with DMSO or U 0126 (20 μ M) for 20 min. At the indicated time points, apoptotic cells were removed and macrophages were washed and biotinylated on ice, and biotinylated proteins were recovered with streptavidin beads and processed for immunoblotting. Recovery of biotinylated proteins was monitored by Ponceau staining of membranes or by Western blotting for integrin $\beta 1$. A representative of three experiments is shown.

Surprisingly, parallel experiments could not confirm a role of ABCA1 in the phagocytosis of apoptotic cells, and this clearly contrasts with previous data (Luciani and Chimini, 1996; Hamon et al., 2000). The reason for the apparent discrepancy is unclear. It could be related to methodological issues. Hamon et al. (2000) quantified uptake of apoptotic cells in macrophages from a small number of mice using ^{51}Cr -labeled apoptotic cells. This method may not distinguish between apoptotic cells that have been ingested by phagocytes or are adherent to the phagocytes. Although more tedious, both microscopic methods used herein count only apoptotic cells clearly within phagocytes or LAMP1-positive phagolysosomes.

Bared et al. (2004) identified ABCA1 as a phagosomal protein and suggest a potential role of ABCA1 for phospholipid efflux from the phagosomal compartment. Recent studies in our laboratory have shown that ABCA1 is induced in phagocytes ingesting apoptotic cells, suggesting that ABCA1 might have a role in the disposal of lipids during phagocytosis (Gerbod-Giannone et al., 2006). Together, these studies indicate that ABCA1, although not directly involved in the phagocytosis of apoptotic cells, may help to recover after phagocytosis.

The failure to obtain ABCA7 $-/-$ mice indicates a role of ABCA7 during embryonic development. It is plausible that a defect in the phagocytosis of apoptotic cells could lead to embryonic lethality, and several knockout mice for other proteins involved in the phagocytosis of apoptotic cells are lethal, notably the LRP1 and calreticulin knockout mice (Herz et al., 1992; Rauch et al., 2000). In contrast to our findings, a recent report by Kim et al. (2005) found a Mendelian genotype distribution in a different line of ABCA7 $-/-$ mice. One difference in the targeting strategies is that our mice have a β -gal gene inserted into the locus so that production of any functional protein is unlikely, whereas Kim et al. (2005) used a replacement vector that could perhaps lead to the formation of small amounts of active protein products. The targeting vector in our mice is multicistronic with an internal ribosome entry site upstream of the LacZ sequence and, thus, a fusion protein of ABCA7 and Lac Z is unlikely to be formed. However, we cannot rule out completely the production of a dominant-negative ABCA7 peptide upstream of the LacZ-Neo-Cassette, which would not be detectable by our antibody. However, the proportionate reduction in the PI resulting from gene targeting and knock down by multiple siRNAs makes this unlikely.

ABCA7 was shown to be important for ERK phosphorylation (Fig. 7), which in turn is required for efficient phagocytosis of apoptotic cells but not for FcR-mediated phagocytosis (Fig. 8 a). Osada et al. (2006) showed a role for both ERK and p38 MAPK signaling in the phagocytosis of apoptotic cells by Sertoli cells but no effect on the phagocytosis of latex beads. For FcR-mediated phagocytosis, ERK activation has been shown to be required in human neutrophils (Mansfield et al., 2000) but not in macrophages (Karimi and Lennartz, 1998). This suggests involvement of different MAPK signaling pathways depending on cell type and phagocytic mechanism. The requirement of ERK activation for phagocytosis may be related to the involvement of ERK in the control of actin reorganization (Kutsuna et al., 2004), the regulation of focal adhesion disassembly (Orr et al., 2002), or cell spreading and migration (Ogura and Kitamura, 1998; Stahle et al., 2003).

The reduced ERK phosphorylation upon stimulation with C1q indicates defective signaling through LRP1. ERK phosphorylation after activation of LRP1 has been shown using thrombospondin binding to calreticulin and after stimulation of LRP1 with connective tissue growth factor (Orr et al., 2003, 2004; Yang et al., 2004). As C1q also binds to calreticulin, the signaling pathway may be similar to the one reported for thrombospondin, calreticulin, and LRP1.

Stimulation of macrophages with apoptotic cells increases ABCA7 and LRP1 levels in the cell surface of ABCA7 $+/+$ macrophages, and this response is markedly reduced in ABCA7 $+/-$ cells (Fig. 6 a). Similarly, stimulation of LRP1 with C1q results in an enrichment of ABCA7 and LRP1 in the cell surface (Fig. 6 b), and this increase is almost abolished in ABCA7 $+/-$ macrophages. ABCA7 may be involved in the trafficking of ABCA7 and LRP1, and this may depend at least in part on ERK phosphorylation as indicated by the abolished increase of ABCA7 and LRP1 in the cell surface after inhibition of ERK phosphorylation (Fig. 8 b). The increase of ABCA7 and LRP1 in ABCA7 $+/+$ macrophages and its failure in ABCA7 $+/-$

cells raises the possibility of a positive-feedback loop. That is, ABCA7 enables maximal LRP1-dependent ERK phosphorylation, which in turn leads to increased expression of ABCA7 and LRP1 at the cell surface, further increasing LRP1 signaling. This model indicating that ABCA7 is required for optimal function of LRP1 may also explain why ABCA7, analogous to LRP1 (Ogden et al., 2001), is only required for the phagocytosis of apoptotic cells but not for FcR-mediated phagocytosis.

On a more fundamental level, the putative role of ABCA7 in signaling events during the phagocytosis of apoptotic cells may be related to an underlying lipid translocase activity. Based on our previous finding that ABCA7 can promote efflux of phosphatidylcholine and sphingomyelin from cells to apoA-I (Wang et al., 2003), we hypothesize that ABCA7 could be involved in the translocation of phospholipids from the inner to the outer leaflet of the plasma membrane, as it has been shown for ABCB4 or MDR2 (multidrug resistance 2; Ruetz and Gros, 1994). Such a "floppase" activity could lead to the formation of specialized membrane microdomains, which may be important for the clustering of receptors and signaling molecules such as LRP1 in the phagocytic cup.

In summary, the data herein show that ABCA7 but not -A1 is required for efficient phagocytosis of apoptotic cells. The functional properties of ABCA7, together with the sequence similarity to CED-7, suggest that ABCA7 may be a mammalian orthologue of CED-7. Mechanistically, ABCA7 is important for maximal and sustained ERK phosphorylation, which in turn is shown to be essential for the phagocytosis of apoptotic cells. At least in part this is explained by the role of ABCA7 in optimal ligand-induced signaling through LRP1 (Fig. 7). These findings shed new light on the fundamental issue of the phagocytosis of apoptotic cells in mammals.

Materials and methods

Reagents and antibodies

1 mg/ml of purified human C1q was obtained from Quidel Corp. The antibody against ABCA7 has been described previously (Wang et al., 2003). Antibody against ABCA1 was from Novus. The antibody against LRP1 for immunoblotting was provided by J. Herz (University of Texas Southwestern Medical Center, Dallas, TX). The anti-integrin β 1 subunit antibody was provided by E.E. Marcantonio (Columbia University, New York, NY). For fluorescence microscopy of LRP1, monoclonal antibodies 5A6 and/or 8B8 (Molecular Innovations) were used. Rat anti-mouse monoclonal antibody (clone 1D4B) against LAMP1 was obtained from BD Biosciences. Antibody against phospho-ERK1/2 and total ERK were obtained from Cell Signaling.

Animals

For the siRNA experiments, C57/B6 mice from The Jackson Laboratory or Taconic were used. ABCA1 heterozygous mating pairs were obtained from The Jackson Laboratory. ABCA7-null/LacZ knockin heterozygous mice were provided by G. Gao (Lilly Research Laboratories, Indianapolis, IN). Originally, these mice were generated by Deltagen, Inc. For in vivo experiments, mice were in C57/B6 background (total number of backcrosses, $n = 10$). ABCA7 +/- mice were obtained by breeding ABCA7 +/+ females with ABCA7 +/- males. The genotype distribution in the offspring was as expected with ~50% ABCA7 +/+ and 50% ABCA7 +/- . Animal protocols were approved by the Institutional Animal Care and Use Committee of Columbia University and the National Jewish Medical and Research Center, respectively.

Cell culture and RNAi

Thioglycollate-elicited mouse peritoneal macrophages were plated in 24-well plates and maintained in DME with 10% (vol/vol) heat-inactivated

FBS, penicillin, and streptomycin under a humidified atmosphere of 90% air and 10% CO₂. Control siRNA1 was designed by scrambling the sequence of a siRNA targeting mouse ABCA7 (control siRNA1, 5'-AAAACCTCCGAC-TACCGAAACT-3'), and control siRNA2 was obtained from QIAGEN (control siRNA2, 5'-AATTCTCCGAACGTGTCACGT-3'). Three siRNA targeting mouse ABCA7 (mABCA7) were used (mABCA7 siRNA1, CAGGGACTTG-ACCAAGGTTTA; mABCA7 siRNA2, 5'-GCCTTCCTAGCTATGCAGACT-3'; mABCA7 siRNA3, 5'-AAGGCCGTGGTGCCTGAGAAA-3') and two siRNA targeting mouse ABCA1 (mABCA1) were used (mABCA1 siRNA1, 5'-TCGGTTGACATCATAAATAT-3'; mABCA1 siRNA2, 5'-CTGGATGATA-ATGAGCAGTA-3'). Transfection with siRNA diluted in Opti-MEM 1 at a concentration of 180 nmol was performed using Oligofectamine (Invitrogen). 1 d after transfection, medium was changed. If RNAi was done for ABCA1, cells were grown in the presence of 2 μ M TO901317 (Sigma-Aldrich) for the last 48 h.

Isolation of human neutrophils and induction of apoptosis

Healthy adult human subjects donated 400 ml of whole blood under a protocol approved by the National Jewish Medical and Research Center's institutional review board. Neutrophils were separated as described previously (Haslett et al., 1985). Before phagocytosis, the cells were irradiated at 312 nm (Fotodyne, Inc.) for 10 min and then cultured in RPMI with 1% BSA at 5×10^6 cells per ml at 37°C plus 5% CO₂ for 2–3 h to induce apoptosis.

Immunoblot analysis

Immunoblot analysis was performed as described previously (Linsel-Nitschke et al., 2005). Relative intensities of bands were determined by densitometry.

In vitro phagocytosis and ruffling experiments

For RNAi experiments, macrophages were plated at 0.5×10^6 cells per well, and for all other experiments, cells were plated at $0.1-0.2 \times 10^6$ per well (24-well plates). Phagocytosis experiments were done 2 d after RNAi or 2 d after harvesting of cells (if no RNAi was performed). If not otherwise indicated, phagocytosis assays were performed with human neutrophils. For some experiments, Jurkat T cells were used. For experiments with C1q-coated apoptotic cells, Jurkat T cells were incubated with 10 μ g/ml C1q followed by spin down and uptake of cells in new medium. Uptake conditions and assessment were almost identical as previously described (Fadok et al., 1998). In brief, apoptotic cells were taken up in DME with 10% FBS and 10^6 cells were added to macrophages in 24-well plates. After 90 min, cells were washed twice in PBS before they were fixed and stained with modified Wright's Giemsa. Using 40 \times light microscopy, macrophages were examined for uptake of apoptotic cells by counting triplicate or quadruplicate wells (200 macrophages/well) in a blinded fashion. The PI was calculated as the number of cells ingested per the total number of macrophages \times 100. For measurement of uptake of apoptotic Jurkat T cells into LAMP1-positive phagolysosomes, Jurkat T cells were prelabeled with Cell-Tracker red (Invitrogen) according to the manufacturer's instructions before induction of apoptosis by UV radiation, and apoptotic cells were incubated with macrophages for 45 min before samples were stained as indicated in the following section. For FcR-mediated phagocytosis, neutrophils were incubated with mouse anti-human CD18 monoclonal antibody (Immunotech), 10 μ l per 10^6 cells (0.2 μ g/ μ l), for 2–3 h. If Jurkat T cells were used they were coated with mouse anti-human CD3 (BD Biosciences). Phagocytosis assays with IgG-coated 4- μ m Aldehyde/Sulfate latex beads (Invitrogen) were performed as previously reported (Booth et al., 2002). J774 macrophages were used for the experiments using PD 98059 (preincubation for 20 min, 20 μ M) and U 0126 (preincubation for 20 min, 10 μ M). For ruffling experiments, macrophages were incubated for 4–5 h in serum-free DME medium before stimulation with 0.05 μ g/ml macrophage inflammatory protein 1 α (PeproTech) for 5 min. Quantification of ruffling was performed as described previously (Cox et al., 1997).

Immunofluorescent microscopy

For immunofluorescent microscopy, glass-bottomed cover dishes were used. Experiments were performed as for phagocytosis assays. After washing with PBS, cells were fixed with 3.2% paraformaldehyde, permeabilized with 0.1% Triton X-100, blocked with 10% goat serum in PBS, and incubated with peptide affinity-purified rabbit anti-ABCA7 antibody and/or mouse monoclonal anti-LRP1 antibodies at a dilution of 1:100 for 1 h at room temperature or at 4°C overnight. As a secondary antibody, goat anti-rabbit Cy3 (Jackson ImmunoResearch Laboratories) and/or goat anti-mouse Alexa 488 (Invitrogen) were used. The experiments using latex beads were performed with J744 macrophages. Beads were added for 20 min at 37°C. Confocal pictures were taken at room temperature with imaging medium PBS using a multiphoton, upright confocal microscope

(LSM 510 NLO; Carl Zeiss MicroImaging, Inc.) with a 63×/0.9 water lens (primary acquisition software obtained from Carl Zeiss MicroImaging, Inc.). For fluorescent microscopy, Axiovert 200 (Carl Zeiss MicroImaging, Inc.) with a Plan-Neofluar 63×/1.25 lens was used attached to a camera (Orca ER; Hamamatsu). Brightness was adjusted with Photoshop 6.0 (Adobe).

In vivo phagocytosis assay

In vivo phagocytosis assays were performed exactly as described by Morimoto et al. (2006). For LPS administration, *Escherichia coli* O111: B4 LPS (List Biological Laboratories) was suspended in PBS at a concentration of 2.5 mg/ml. 200 mcg of LPS was instilled intratracheally. 72 h later, bronchoalveolar lavage was performed.

Surface biotinylation and ERK phosphorylation assay

Thioglycollate-elicited mouse peritoneal macrophages were plated in 12-well plates at 1.5×10^6 cells/well. The medium was changed the next day. After 2 d, cells were incubated with apoptotic Jurkat T cells for the indicated time points followed by three washes with ice cold PBS. For ERK phosphorylation assays with clinical grade, 100 µg/ml of aggregated IgG macrophages were cultured for the last 18 h in the presence of 100 U/ml γ interferon followed by incubation for 3–4 h in serum-free DME. For C1q experiments, macrophages were incubated for 3–4 h in serum-free DME before stimulation. Biotinylation was performed with 0.5 mg/ml Sulfo-NHS-SS-Biotin (Pierce Chemical Co.) for 30 min on ice. Cells were lysed on ice, and the lysis buffer was supplemented with Tyr and Ser/Thr phosphatase inhibitor cocktail (Upstate Biotechnology). 100–200 µg of cell lysates were used for pull down with 25 µl of streptavidin beads (Pierce Chemical Co.) followed by two washes in lysis buffer. 25 µg of protein was used for immunoblotting according to the protocol provided with the ERK1/2 antibody.

Data analysis

Data are expressed as means and SD if not otherwise stated. Significance of differences was always calculated with a two-sided unpaired *t* test. For box plots, StatView was used. For pairwise alignments, the program NEEDLE with scoring matrix EBLSOUM40 was used, and for multiple alignments, the ClustalW program was used.

Online supplemental material

Fig. S1 depicts the alignment of CED-7, mouse ABCA7, and ABCA1 amino acid sequences. Fig. S2 shows localization of ABCA7 in phagocytic cups/phagosomes during FcR-mediated phagocytosis. Fig. S3 shows a representative immunoblot for ABCA1 and β -actin after knock down of ABCA1 in peritoneal macrophages. Fig. S4 shows membrane ruffling with quantification of ABCA7 $+/+$ and $+/-$ macrophages after stimulation. Fig. S5 shows immunoblot and quantification of ERK phosphorylation after stimulation of ABCA7 $+/+$ and $+/-$ macrophages with aggregated IgG. Online supplemental material is available at <http://www.jcb.org/cgi/content/full/jcb.200601030/DC1>.

We thank Aretha Townsend for her assistance with breeding and genotyping the different knockout mice and Jennifer Kench for her support in performing the animal studies at the National Jewish Research Center.

This study was supported by National Institutes of Health grants HL22682 and 84555 (to A.R. Tall), GM61031 and PN0503-104 (to P.M. Henson), and HL54164 (to S. Greenberg). A.W. Jehle was supported in part by the Swiss Foundation for Medical-Biological Grants and the Novartis Foundation.

The authors have no conflicting financial interests.

Submitted: 5 January 2006

Accepted: 12 July 2006

References

Aderem, A., and D.M. Underhill. 1999. Mechanisms of phagocytosis in macrophages. *Annu. Rev. Immunol.* 17:593–623.

Bared, S.M., C. Buechler, A. Boettcher, R. Dayoub, A. Sigrüener, M. Grandl, C. Rudolph, A. Dada, and G. Schmitz. 2004. Association of ABCA1 with syntaxin 13 and flotillin-1 and enhanced phagocytosis in tangier cells. *Mol. Biol. Cell.* 15:5399–5407.

Booth, J.W., M.K. Kim, A. Jankowski, A.D. Schreiber, and S. Grinstein. 2002. Contrasting requirements for ubiquitylation during Fc receptor-mediated endocytosis and phagocytosis. *EMBO J.* 21:251–258.

Cox, D., P. Chang, Q. Zhang, P.G. Reddy, G.M. Bokoch, and S. Greenberg. 1997. Requirements for both Rac1 and Cdc42 in membrane ruffling and phagocytosis in leukocytes. *J. Exp. Med.* 186:1487–1494.

deCathelineau, A.M., and P.M. Henson. 2003. The final step in programmed cell death: phagocytes carry apoptotic cells to the grave. *Essays Biochem.* 39:105–117.

Fadok, V.A., M.L. Warner, D.L. Bratton, and P.M. Henson. 1998. CD36 is required for phagocytosis of apoptotic cells by human macrophages that use either a phosphatidylserine receptor or the vitronectin receptor (alpha v beta 3). *J. Immunol.* 161:6250–6257.

Gardai, S.J., K.A. McPhillips, S.C. Frasch, W.J. Janssen, A. Starefeldt, J.E. Murphy-Ullrich, D.L. Bratton, P.A. Oldenborg, M. Michalak, and P.M. Henson. 2005. Cell-surface calreticulin initiates clearance of viable or apoptotic cells through trans-activation of LRP on the phagocyte. *Cell.* 123:321–334.

Gardai, S.J., Y.Q. Xiao, M. Dickinson, J.A. Nick, D.R. Voelker, K.E. Greene, and P.M. Henson. 2003. By binding SIRPalpha or calreticulin/CD91, lung collectins act as dual function surveillance molecules to suppress or enhance inflammation. *Cell.* 115:13–23.

Gerbod-Giannone, M.C., Y. Li, A. Holleboom, S. Han, L.C. Hsu, I. Tabas, and A.R. Tall. 2006. TNFalpha induces ABCA1 through NF-kappaB in macrophages and in phagocytes ingesting apoptotic cells. *Proc. Natl. Acad. Sci. USA.* 103:3112–3117.

Hamon, Y., C. Broccardo, O. Chambenoit, M.F. Luciani, F. Toti, S. Chaslin, J.M. Freyssinet, P.F. Devaux, J. McNeish, D. Marguet, and G. Chimini. 2000. ABC1 promotes engulfment of apoptotic cells and transbilayer redistribution of phosphatidylserine. *Nat. Cell Biol.* 2:399–406.

Haslett, C., L.A. Guthrie, M.M. Kopaniak, R.B. Johnston Jr., and P.M. Henson. 1985. Modulation of multiple neutrophil functions by preparative methods or trace concentrations of bacterial lipopolysaccharide. *Am. J. Pathol.* 119:101–110.

Henson, P.M., D.L. Bratton, and V.A. Fadok. 2001. Apoptotic cell removal. *Curr. Biol.* 11:R795–R805.

Herz, J., and D.K. Strickland. 2001. LRP: a multifunctional scavenger and signaling receptor. *J. Clin. Invest.* 108:779–784.

Herz, J., D.E. Clouthier, and R.E. Hammer. 1992. LDL receptor-related protein internalizes and degrades uPA-PAI-1 complexes and is essential for embryo implantation. *Cell.* 71:411–421.

Karimi, K., and M.R. Lennartz. 1998. Mitogen-activated protein kinase is activated during IgG-mediated phagocytosis, but is not required for target ingestion. *Inflammation.* 22:67–82.

Kim, W.S., M.L. Fitzgerald, K. Kang, K. Okuhira, S.A. Bell, J.J. Manning, S.L. Koehn, N. Lu, K.J. Moore, and M.W. Freeman. 2005. Abca7 null mice retain normal macrophage phosphatidylcholine and cholesterol efflux activity despite alterations in adipose mass and serum cholesterol levels. *J. Biol. Chem.* 280:3989–3995.

Kinchen, J.M., J. Cabello, D. Klingele, K. Wong, R. Feichtinger, H. Schnabel, R. Schnabel, and M.O. Hengartner. 2005. Two pathways converge at CED-10 to mediate actin rearrangement and corpse removal in *C. elegans*. *Nature.* 434:93–99.

Kutsuna, H., K. Suzuki, N. Kamata, T. Kato, F. Hato, K. Mizuno, H. Kobayashi, M. Ishii, and S. Kitagawa. 2004. Actin reorganization and morphological changes in human neutrophils stimulated by TNF, GM-CSF, and G-CSF: the role of MAP kinases. *Am. J. Physiol. Cell Physiol.* 286:C55–C64.

Linsel-Nitschke, P., A.W. Jehle, J. Shan, G. Cao, D. Bacic, D. Lan, N. Wang, and A.R. Tall. 2005. Potential role of ABCA7 in cellular lipid efflux to apoA-I. *J. Lipid Res.* 46:86–92.

Luciani, M.F., and G. Chimini. 1996. The ATP binding cassette transporter ABC1, is required for the engulfment of corpses generated by apoptotic cell death. *EMBO J.* 15:226–235.

Mansfield, P.J., J.A. Shayman, and L.A. Boxer. 2000. Regulation of polymorphonuclear leukocyte phagocytosis by myosin light chain kinase after activation of mitogen-activated protein kinase. *Blood.* 95:2407–2412.

Marguet, D., M.F. Luciani, A. Moynault, P. Williamson, and G. Chimini. 1999. Engulfment of apoptotic cells involves the redistribution of membrane phosphatidylserine on phagocyte and prey. *Nat. Cell Biol.* 1:454–456.

Morimoto, K., W.J. Janssen, M.B. Fessler, K.A. McPhillips, V.M. Borges, R.P. Bowler, Y.Q. Xiao, J.A. Kench, P.M. Henson, and R.W. Vandivier. 2006. Lovastatin enhances clearance of apoptotic cells (efferocytosis) with implications for chronic obstructive pulmonary disease. *J. Immunol.* 176:7657–7665.

Ogden, C.A., A. deCathelineau, P.R. Hoffmann, D. Bratton, B. Ghebrehiwet, V.A. Fadok, and P.M. Henson. 2001. C1q and mannose binding lectin engagement of cell surface calreticulin and CD91 initiates macrophagocytosis and uptake of apoptotic cells. *J. Exp. Med.* 194:781–795.

Ogura, M., and M. Kitamura. 1998. Oxidant stress incites spreading of macrophages via extracellular signal-regulated kinases and p38 mitogen-activated protein kinase. *J. Immunol.* 161:3569–3574.

Orr, A.W., M.A. Paller, and J.E. Murphy-Ullrich. 2002. Thrombospondin stimulates focal adhesion disassembly through Gi- and phosphoinositide 3-kinase-dependent ERK activation. *J. Biol. Chem.* 277:20453–20460.

- Orr, A.W., C.E. Pedraza, M.A. Pallero, C.A. Elzie, S. Goicoechea, D.K. Strickland, and J.E. Murphy-Ullrich. 2003. Low density lipoprotein receptor-related protein is a calreticulin coreceptor that signals focal adhesion disassembly. *J. Cell Biol.* 161:1179–1189.
- Orr, A.W., M.A. Pallero, W.C. Xiong, and J.E. Murphy-Ullrich. 2004. Thrombospondin induces RhoA inactivation through FAK-dependent signaling to stimulate focal adhesion disassembly. *J. Biol. Chem.* 279:48983–48992.
- Osada, Y., A. Shiratsuchi, and Y. Nakanishi. 2006. Involvement of mitogen-activated protein kinases in class B scavenger receptor type I-induced phagocytosis of apoptotic cells. *Exp. Cell Res.* 312:1820–1830.
- Rauch, F., J. Prud'homme, A. Arabian, S. Dedhar, and R. St-Arnaud. 2000. Heart, brain, and body wall defects in mice lacking calreticulin. *Exp. Cell Res.* 256:105–111.
- Reddien, P.W., and H.R. Horvitz. 2004. The engulfment process of programmed cell death in *Caenorhabditis elegans*. *Annu. Rev. Cell Dev. Biol.* 20:193–221.
- Ruetz, S., and P. Gros. 1994. Phosphatidylcholine translocase: a physiological role for the *mdr2* gene. *Cell.* 77:1071–1081.
- Stahle, M., C. Veit, U. Bachfischer, K. Schierling, B. Skripczynski, A. Hall, P. Gierschik, and K. Giehl. 2003. Mechanisms in LPA-induced tumor cell migration: critical role of phosphorylated ERK. *J. Cell Sci.* 116:3835–3846.
- Su, H.P., K. Nakada-Tsukui, A.C. Tosello-Trampont, Y. Li, G. Bu, P.M. Henson, and K.S. Ravichandran. 2002. Interaction of CED-6/GULP, an adapter protein involved in engulfment of apoptotic cells with CED-1 and CD91/low density lipoprotein receptor-related protein (LRP). *J. Biol. Chem.* 277:11772–11779.
- Taylor, P.R., A. Carugati, V.A. Fadok, H.T. Cook, M. Andrews, M.C. Carroll, J.S. Savill, P.M. Henson, M. Botto, and M.J. Walport. 2000. A hierarchical role for classical pathway complement proteins in the clearance of apoptotic cells in vivo. *J. Exp. Med.* 192:359–366.
- Teder, P., R.W. Vandivier, D. Jiang, J. Liang, L. Cohn, E. Pure, P.M. Henson, and P.W. Noble. 2002. Resolution of lung inflammation by CD44. *Science.* 296:155–158.
- Vandivier, R.W., C.A. Ogden, V.A. Fadok, P.R. Hoffmann, K.K. Brown, M. Botto, M.J. Walport, J.H. Fisher, P.M. Henson, and K.E. Greene. 2002. Role of surfactant proteins A, D, and Clq in the clearance of apoptotic cells in vivo and in vitro: calreticulin and CD91 as a common collectin receptor complex. *J. Immunol.* 169:3978–3986.
- Wang, N., D. Lan, M. Gerbod-Giannone, P. Linsel-Nitschke, A.W. Jehle, W. Chen, L.O. Martinez, and A.R. Tall. 2003. ATP-binding cassette transporter A7 (ABCA7) binds apolipoprotein A-I and mediates cellular phospholipid but not cholesterol efflux. *J. Biol. Chem.* 278:42906–42912.
- Wu, Y.C., and H.R. Horvitz. 1998. The *C. elegans* cell corpse engulfment gene *ced-7* encodes a protein similar to ABC transporters. *Cell.* 93:951–960.
- Yang, M., H. Huang, J. Li, D. Li, and H. Wang. 2004. Tyrosine phosphorylation of the LDL receptor-related protein (LRP) and activation of the ERK pathway are required for connective tissue growth factor to potentiate myofibroblast differentiation. *FASEB J.* 18:1920–1921.